Analytica Chimica Acta 1198 (2022) 339510

Contents lists available at ScienceDirect

Analytica Chimica Acta

journal homepage: www.elsevier.com/locate/aca

Dual amplification enabled counting based ultrasensitive enzyme-linked immunosorbent assay

Haomin Liu [a], Yu Lei [a, b, *]

[a] Department of Chemical and Biomolecular Engineering, University of Connecticut, Storrs, CT, 06269, USA
[b] Department of Biomedical Engineering, University of Connecticut, Storrs, CT, 06269, USA

HIGHLIGHTS

- Ultrasensitive ELISA was developed based on a new dual amplification enabled counting strategy.
- Dural amplification was realized through the combination of tyramide signal amplification (TSA) and alkaline phosphatase enabled formation of fluorescent precipitates.
- This study opens a new and universal avenue to improve the sensitivity of conventional plate-based ELISA.

GRAPHICAL ABSTRACT

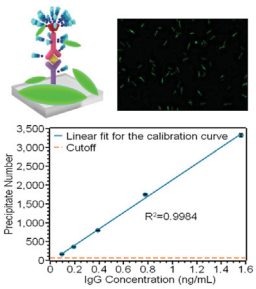

ARTICLE INFO

Article history:
Received 14 October 2021
Received in revised form
12 January 2022
Accepted 14 January 2022
Available online 18 January 2022

Keywords:
ELISA
Counting
Dual amplification
Scanning
Ultrasensitivity

ABSTRACT

ELISA is a predominant technique in the detection of biomarkers. Notwithstanding its ubiquity and numerous advantages, its application for detection of low abundant biomarkers requires the ultrasensitivity. To bridge the gap between the need and availability, an innovative dual amplification enabled counting based ELISA was developed for ultrasensitive detection of mouse total IgG (a model biomarker). The dual amplification strategy, which is compatible with conventional plate-based ELISA, was realized through tyramide signal amplification (TSA) and alkaline phosphatase enabled formation of fluorescent precipitates. The counting of fluorescent precipitates in 25 images of each well can correlate the number of precipitates to the concentration of IgG with good linearity and lower the limit of detection of the commercial mouse IgG kit (1.56 ng/mL) to 54.5 pg/mL. Recovery tests further demonstrate the reliability of the developed method. This study opens a new avenue to improve the sensitivity of conventional plate-based ELISA.

1. Introduction

Immunoassay has been a dominant technique in biomarker detection since its emergence in the 1960s [1]. Specifically, enzyme-linked immunosorbent assay (ELISA) developed in 1971 rapidly becomes the gold standard for detecting biomolecules [2,3]. Because of its convenience and wide applications in various fields, the improvement of ELISA performance started nearly at the same time when it was developed, which was witnessed by fluorescence-based ELISA developed in 1979 [2] and beads-based ELISA employed to detect antigens by Gundersen in 1991 [4]. In the past two decades, a variety of ELISAs in different variants have been further reported, including the digital ELISA for biomarker detection at a single molecule level [5–7], paper-based ELISA for fast

* Corresponding author. Department of Chemical and Biomolecular Engineering, University of Connecticut, Storrs, CT, 06269, USA.
E-mail address: yu.lei@uconn.edu (Y. Lei).

https://doi.org/10.1016/j.aca.2022.339510
0003-2670/

diagnosis and low-cost point of care [8,9], and nano-ELISA for food analysis [10,11]. ELISA was also recently adapted to detect emerging targets such as SARS-CoV-2 [12,13]. Although the aforementioned ELISA variants offer additional options to end-users, the dominant ELISA format employed in the clinical practice is still conventional plate-based ELISA because of its low instrument requirements, high reliability, affordability, adaptability, and convenience. However, conventional plate-based ELISAs typically detect the concentration of biomarkers at the level of 10^{-12} M and above [14], and thus are not able to offer the required limit of detection (LOD) for early diagnosis of disease-related biomarkers (e.g., HIV and cancers) [15,16]. Therefore, there is a high demand to improve the conventional plate-based ELISA in order to diagnose the fatal diseases at their early stages.

It is always challenging to improve the performance of conventional plate-based ELISA with minimal modifications of the protocol, which can be immediately adapted to the clinical practice using the commercially available ELISA kits. One research direction is to introduce nanoparticles (e.g., metal nanoparticles, silicon nanoparticles, biological nanoparticles, etc.) into current conventional plate-based ELISA for signal enhancement [17–19]. The major merit of this strategy is to enhance the signal intensity through these nanoparticles enabled a large number of reporter enzymes. For example, Lu et al. designed a Pt/IrO_2@streptavidin nano flower as a reporting enzyme carrier to enrich the quantities of horseradish peroxidase (HRP), which would help produce more colored products in the final signal generation step with a short time [20]. Recently, we employed engineered outer membrane vesicles (OMVs) decorated with Z domain and a number of Nanoluc (Nluc) luciferases to generate bioluminescence signal for IgG detection [21]. Although the nanoparticles-based strategy is elegant, some disadvantages such as the requirement of nanoparticles and the variation of nanoparticles' quality from batch to batch may result in low reproducibility, thus prohibiting their wide applications. The other research direction is to develop new substrate molecules for enhanced signals. For example, Acharya et al. demonstrated that hydrocyanines could be employed as the substrate for HRP, which increased the sensitivity of conventional ELISAs by two orders of magnitude [22]. However, its application in plate-based ELISA does not receive extensive attention, which is presumably ascribed to the fact that the new substrates are not easily accessible and the synthesis of substrate causes extra cost. Therefore, a new method compatible with conventional plate-based ELISA is still highly demanded.

In this study, we developed a new dual amplification approach to take the advantages of enriching the quantities of reporting enzymes through tyramide signal amplification (TSA) and introducing an alkaline phosphatase (ALP) enabled fluorescent precipitate reporting system into a conventional plate-based ELISA, thus allowing direct-counting based ultrasensitive detection of biomarkers. TSA was first developed in 1989 for immunoassay's signal amplification [23]. Because of its low cost, fast turnaround, high reliability, and convenience, TSA has been introduced in *in-situ* hybridization, electron microscopic immunocytochemistry, cell labeling, tissue signal amplification, etc., for low abundant biomolecules of interest [24–26]. Nowadays, TSA has also been one of the prevailing signal amplification methods in designing innovative ELISAs, including quantum dots conjugated with tyramide as reporters for ELISA of IgG detection [27] and integration of TSA with fibrin hydrogels to develop a simplified CARD-digital ELISA for Interleukin-6 with the LOD as low as 1 fM [28]. However, they are not compatible with conventional plate-based ELISA platforms in general. On the other hand, ELF 97 phosphate substrate (ELFP) [29] has been extensively employed as the substrate of ALP. The product of this enzyme reaction is ELF alcohol (ELFA) that yields a bright green fluorescent precipitate with an extremely large Stokes shift (λ_{ex} = 345 nm and λ_{em} = 530 nm). The signal could be easily distinguished from the cellular autofluorescence, which enables it to acquire extensive usage in cell staining [30–33]. Recently, we revealed that the ELFA tended to form large precipitates in basic environments and then integrated ALP-enabled ELFA fluorescent precipitates reporting system with whole area scanning (WAS) technology to investigate the blocking efficiency of three blocking agents in conventional plate-based ELISA through a digital-counting method [34]. It shows the potential to be applied in the conventional plate-based ELISA.

Herein, an innovative dual amplification enabled counting based ELISA (DAC-ELISA) was developed for ultrasensitive detection of mouse total IgG (a model biomarker). Conventional sandwich immunocomplex constructed in the microplate wells was employed as a base. The dual amplification strategy, which is compatible with conventional plate-based ELISAs, was accomplished through tyramide signal amplification and ALP-enabled formation of fluorescent precipitates. The first amplification relies on biotinyl-tyramide (B-T) conjugating with the sandwich immunocomplex (triggered by HRP) to increase the number of biotins, which will further increase the number of reporting enzymes (ALP) through the interaction between biotin and Streptavidin-ALP (SA-ALP), thus resulting in the second amplification through rapid fluorescent precipitates formation upon the addition of ELFA-saturated ELFP substrate. The rapid counting of fluorescent precipitates in 25 images of each well can be correlated to the concentration of IgG with an impressive limit of detection (LOD) compared to that of conventional ELISA. Mouse IgG spiked in goat serum samples was investigated to further evaluate its specificity, recovery, accuracy, and precision. This study indicates that the developed dual amplification strategy opens a new but universal avenue to improve the sensitivity of conventional plate-based ELISA and holds great potential in achieving ultrasensitive detection of biomarkers on conventional plate-based ELISA platforms.

2. Experimental section

2.1. Reagents, supplies, and instruments

IgG (Total) Mouse Uncoated ELISA Kit, Streptavidin-Alkaline phosphatase conjugate (SA-ALP), and ELF™ 97 phosphate (ELFP) were purchased from Thermo Fisher Scientific Inc. (USA). ELAST ELISA Amplification Kit was purchased from PerkinElmer Life Sciences, Inc. (USA). Bovine Serum Albumin (BSA) was bought from Sigma-Aldrich (USA). 10 × phosphate buffered saline (PBS, pH = 7.4) and 10 × Tris/Glycine/SDS buffer (pH = 8.3) were acquired from Bio-Rad Laboratories, Inc. (USA). 10 × buffers were diluted to 1 × before use. H_3PO_4, Goat Serum, Tween™ 20, Syringe Filters (pore size, 0.2 μm), and Falcon™ 96-well (flat bottom) polystyrene microplates were purchased from Fisher Scientific Company (USA). Colorimetric readouts were acquired using Synergy™ HT Multi-Detection Microplate Reader (Bio-Tek Instruments). Images were captured using the BZ-X800 All-in-One fluorescence microscope (Keyence Corporation) with a 20 × objective lens (NA = 0.45, Nikon). Customized optical filter cube with λ_{ex} = 345 nm and λ_{em} = 530 nm was obtained from Chroma Technology Corporation. All images were processed using the BZ-X800 analyzer software.

2.2. Protocol of DAC-ELISA

The procedure of DAC-ELISA consists of 4 major steps in sequence, including a traditional sandwich ELISA step, a TSA step, an ALP enabled ELF amplification step, and image capture for direct-counting.

2.2.1. The sandwich ELISA step

The protocol used here was adapted from the manual of the purchased ELISA kit. In brief, 100 μL capture antibody solution was added to each well of the 96-well microplate. The plate was sealed and incubated overnight at 4 °C. After overnight incubation, solutions were aspirated, the capture antibody coated wells were washed twice using 300 μL wash buffer (1 × PBS, 0.05% Tween™ 20). After washing, all wells were blocked with 250 μL blocking buffer provided in the ELISA kit for 2 h at room temperature. The blocking solution was then aspirated, and all wells were washed twice using the wash buffer. Next, 100 μL analyte dissolved in assay buffer (a component of the ELISA kit) with varying concentrations was added into the well, denoted as experimental wells, while 100 μL assay buffer was loaded into the control wells. After the addition of analyte dissolved in assay buffer and blank assay buffer, 50 μL HRP conjugated detection antibody solution was added into each well. The plate was incubated for 2 h at room temperature. Then, the solutions were aspirated, and wells were washed with wash buffer for four times.

2.2.2. TSA step

The protocol used here was adapted from the manual of the amplification kit. Wells prepared in the sandwich ELISA were incubated with biotinyl-tyramide (B-T) solution (5 μL/mL) in the presence of H_2O_2 for 15 min at room temperature. After aspiration, all wells were washed with 1 × PBS, 0.5% Tween™ 20 for four times.

2.2.3. ALP-enabled ELF amplification

Wells prepared in sandwich ELISA followed by TSA were then incubated with 100 μL of 2 μg/mL SA-ALP dissolved in PBS with 1% BSA for 15 min at room temperature. Solutions were aspirated, and all wells were washed using 1 × PBS, 0.5% Tween™ 20 for four times. After washing, 100 μL of 16.67 μM ELFP Tris/Glycine/SDS solution (ELFA saturated) was added into each well. The plate was incubated for 2.5 h at room temperature before image capture.

2.2.4. Image capture for direct-counting

The microplate was fixed on the stage of the BZ-X800 microscope for imaging. For each well of interest, 25 images were captured, and the number of ELFA precipitates in each image was counted employing BZ-X800 analyzer software.

2.3. Optimization of B-T concentration for TSA

Wells were first prepared employing the sandwich ELISA protocol, and the analyte dissolved in assay buffer were 2-fold serial diluted mouse IgG standard (a component of the ELISA kit) from 1.5625 ng/mL to 0.0977 ng/mL. Wells prepared in sandwich ELISA were then incubated with 50 × (20 μL B-T solution/mL), 100 × (10 μL/mL), 200 × (5 μL/mL) diluted B-T solutions in the kit for 15 min at room temperature. After aspiration, all wells were washed with 1 × PBS, 0.5% Tween™ 20 for four times. After washing, each well was incubated with 100 μL SA-HRP (a component of the ELISA amplification kit) for 15 min at room temperature. All wells were then aspirated and washed using 1 × PBS, 0.5% Tween™ 20 for four times. Finally, wells were incubated with 100 μL TMB substrate solution for 15 min at room temperature. 100 μL of 1 M H_3PO_4(aq) was finally added to quench the reaction. The plate was read at 450 nm employing a microplate reader. Experiments were conducted in triplicate. The optimal B-T concentration (5 μL/mL) which was experimentally determined to generate the best amplification was employed in TSA in this study.

2.4. Optimization of the substrate

2.4.1. Preparation of ELFA-Saturated ELFP solution

100 μL of 100 μM ELFP Tris/Glycine/SDS solution was mixed with 100 μL of 2 μg/mL SA-ALP dissolved in 1 × PBS with 1% BSA for 15 min. Then, the mixture was incubated in a 100 °C water bath for 1 h to inactivate the ALP. The temperature was reduced to room temperature before further use. ALP inactivated mixture was vortexed for 30 s. 100 μL mixture was then added to 4900 μL ELFP Tris/Glycine/SDS solution where the final concentration of ELFP is 16.67 μM. This solution was incubated for 10 min and then filtered with a 0.2 μm syringe filter to separate un-dissolved ELFA precipitates. The filtrate obtained was an ELFA-saturated ELFP solution, which was ready for use.

2.4.2. The effect of ELFA saturation in ELFP solution on fluorescent precipitates formation

Two wells were prepared employing the DAC-ELISA protocol. The analyte dissolved in assay buffer was 100 μL of 1.5625 ng/mL mouse IgG standard (a component of the ELISA kit). Modifications were in the ELF amplification step where one well was incubated with 100 μL of 16.67 μM ELFP Tris/Glycine/SDS solution (ELFA saturated), and the other was incubated with 100 μL of 16.67 μM ELFP Tris/Glycine/SDS solution. Images were captured every 30 min during 3 h incubation. Experiments were conducted in triplicate.

2.4.3. Determination of optimal ELFP concentration

Wells were prepared employing the DAC-ELISA protocol. The test was based on a 100 μL assay buffer for background signal as minimal background signal is critical for improving the limit of detection. Modifications were in the ELF amplification step where wells were incubated with 100 μL of 50 μM, 25 μM, 16.67 μM, and 12.5 μM ELFP Tris/Glycine/SDS solution (ELFA saturated), respectively. Experiments were conducted in triplicate.

2.4.4. Determination of optimal incubation time

Wells were prepared employing the DAC-ELISA protocol. The analyte dissolved in assay buffer was 100 μL of 1.5625 ng/mL mouse IgG standard in the ELISA kit. Modifications appeared in the image capture step, where images were captured every 30 min during 4 h of incubation. Experiments were conducted in triplicate.

2.5. Matrix effect and recovery test

For the study of the matrix effect, wells were prepared employing the DAC-ELISA protocol. The analyte was 100 μL diluted goat serum in assay buffer. Goat serum was diluted 4, 10, 100, 500, 1,000, 10,000, and 100,000 folds using the assay buffer. In the recovery test, wells were prepared employing the DAC-ELISA protocol. For the study of the recovery test, the analyte was 100 μL of IgG standard spiked into 100,000 times diluted goat serum in assay buffer where the final concentrations of IgG standard are 0.1 ng/mL and 0.2 ng/mL, respectively.

3. Results and discussion

3.1. Principle of dual amplification enabled counting (DAC) based system for conventional sandwich ELISA

DAC system consists of two amplification steps, including TSA and ALP-enabled ELF signal amplification (Fig. 1). TSA is a widely used signal amplification strategy and ideal for the detection of biomolecules with low abundance. The principle of TSA utilized in this study is illustrated in Fig. S1. In the presence of H_2O_2, B-T is oxidized by HRPs, which have already been conjugated on the

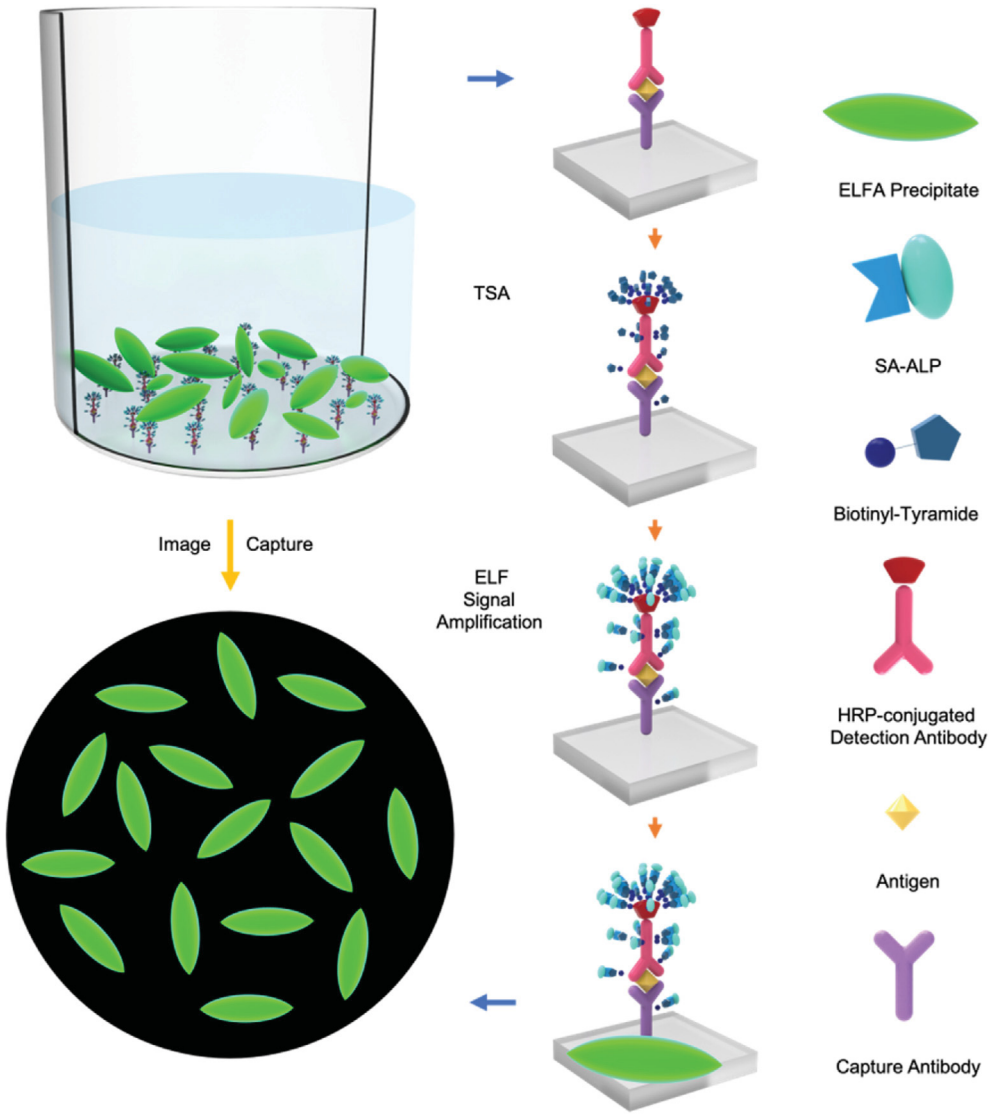

Fig. 1. The principle of the dual amplification enabled counting based ELISA (DAC-ELISA) system.

detection antibody, to form tyramide radicals. These radicals further react with electron-enriched molecules such as tryptophan and tyrosine on biomolecules (e.g., proteins, antibodies, etc.) in the proximity. As this reaction has no selectivity, it labels the detection antibody, antigens, and capture antibody in proximity with biotin.

To generate the signal, ALP-enabled ELF signal amplification is introduced after TSA, and the corresponding reaction is illustrated in Fig. S2. As shown in Fig. 1, the more biotins are conjugated onto the immunocomplex; the more reporting enzymes are anchored through the interaction between biotin and SA-ALP. Upon the addition of the substrate (ELFA-saturated ELFP solution), ALPs convert ELFP to ELFA and form spindle-shaped fluorescent precipitates with superior photostability that can attach to the bottom surface of the plate. The precipitates can be imaged, and their total number can be counted and correlated with the concentration of analytes. In clinical practice, analyte standards can be employed to establish the calibration curve, and thus the concentrations in unknown samples can be obtained accordingly. In this design, the signal is amplified by TSA and ELF amplification in tandem, which significantly lowers the limit of detection of the method, comparing to the conventional ELISA.

Employing an ELFA-saturated ELFP substrate is necessary for this strategy, which shortens the assay time and enhances the sensitivity. Usually, ELFA is produced as ALP catalyzes ELFP substrate. Although ELFA is water-insoluble, it does not precipitate out from the solution until the solution is saturated with ELFA. If only ELFP solution is employed, a different time is required to generate ELFA-saturated solution as the number of ALPs is dependent on the analyte concentration. Since ELFA precipitation starts at different moments, the correlation between ALP and ELFA precipitate cannot be reliably established among different target concentrations. The use of ELFA-saturated ELFP could avoid such differences. Once the ELFA-saturated ELFP is added, the ELFA precipitate will separate from the solvent immediately regardless of the amount of ALP. In addition, the utilization of the ELFA-saturated ELFP substrate can shorten the assay time by eliminating the saturation step, especially important for the detection of the low abundant target. As illustrated in Fig. 2, the number of ELFA precipitate produced from the use of the ELFA-saturated ELFP substrate is more than that of the unsaturated one under the same incubation time. Therefore, an ELFA-saturated ELFP substrate is used in subsequent experiments.

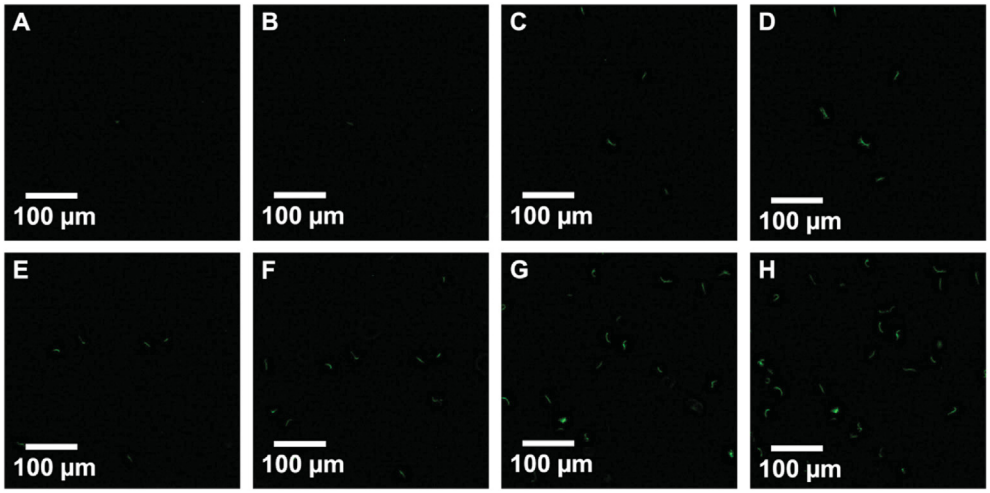

Fig. 2. The comparison of the effect of ELFP substrate and ELFA-saturated ELFP substrate on fluorescent precipitates formation. Representative field-of-view (FOV) image of a well incubated with 16.67 μM ELFP substrate at (A) 1.5 h, (B) 2 h, (C) 2.5 h, and (D) 3 h, respectively. Representative FOV images of a well incubated with 16.67 μM ELFP substrate (ELFA saturated) at (E) 1.5 h, (F) 2 h, (G) 2.5 h, and (H) 3 h, respectively. The analyte was IgG standard with a concentration of 1.5625 ng/mL, and the dual amplification protocol was applied.

3.2. Performance of DAC reporting system in mouse IgG standard test under ELISA format

The main goal of this study aims at developing the DAC-ELISA system to improve the LOD of the conventional plate-based ELISA with a minor modification of the protocol. The LOD of the conventional ELISA kit employed in this study is 1.56 ng/mL. The IgG standards tested in the current study were diluted from 1.56 ng/mL in a 2-fold serial manner, and the wells with blank assay buffer were prepared as negative controls. Parallel tests were conducted employing the original HRP-TMB reporting system, TSA-HRP-TMB reporting system, and DAC reporting system. For the original HRP-TMB reporting system described in the kit (Fig. 3A), all absorbance values obtained at 450 nm were below 0.25. These readouts were so small and close to the cutoff value (0.065 ± 0.002) and the resolution of the microplate reader, indicating that the detection of IgG lower than 1.56 ng/mL is not achievable using original HRP-TMB system. This observation is in good agreement with the LOD of the kit. For the HRP-TSA-TMB reporting system (Fig. 3B), signals were amplified to a certain extent compared to the HRP-TMB system, which is attributed to TSA. However, the cutoff value (0.183 ± 0.004) increased and was larger than the readout of 0.148 ± 0.019, corresponding to 0.098 ng/mL IgG standard. In addition, no strong linear relationship was observed between the absorbance and the tested concentrations range. These results indicate that these two reporting systems may not be reliable to be applied for biomarker detection at such low concentrations. As shown in Fig. 3C, the DAC reporting system surpassed the other two strategies and lowered the LOD of the conventional ELISA over 25 times. In addition, a good linear fit was achieved for the IgG standards with the concentration ranging from 98 pg/mL to 1.5625 ng/mL. The LOD was 54.5 pg/mL, calculated by extrapolating the concentration from the readout equal to background readout plus three standard deviations of the background readout. The coefficient variations (CV) of all values were ranging from 1.25% to 2.41%, which represented the superior precision and repeatability of the results. Moreover, the large slope of the calibration curve between the precipitate number and the analyte concentration indicates enhanced sensitivity and accuracy since the readout number varies substantially even though the concentration of analyte just has a minor variation (Fig. 3D–I).

3.3. Matrix effect, accuracy, and precision

Elimination of matrix effect is indispensable for all specimens from body fluids such as plasma and serum due to the fact that the complicated components in biological samples might result in high background noise and thus cause overestimated results. Currently, the predominant strategy to eliminate the matrix effect is through direct dilution of the sample into assay buffer. In the commercial mouse IgG ELISA kit, the supplier recommends the starting dilution is 10,000-fold for serum and plasma samples using assay buffer. To evaluate the matrix effect in the current study, goat serum (free of mouse IgG) was employed and diluted in assay buffer provided in the kit from 4 to 100,000 folds. As illustrated in Fig. 4A, the precipitate numbers were decreased with the increase of dilution factors initially, as expected. The average precipitate number with dilution factors of 1,000, 10,000, and 100,000 was counted and calculated to be as low as 10, 19, and 23, respectively. This result indicates that the matrix effect of biological samples could be ignored by a substantial dilution. Thus, 100,000-fold diluted goat serum with spiked mouse IgG is used in subsequent recovery tests. To carry out the recovery tests, the as-developed DAC-ELISA was challenged with 100,000-fold diluted goat serum spiked with 0.1 ng/mL and 0.2 ng/mL mouse IgG, respectively. The results of the IgG standard spiked goat serum test ($n = 3$) show superior accuracy, precision, and recovery (Fig. 4B). For the 0.2 ng/mL and 0.1 ng/mL samples tested, the recovery reached $99.35 \pm 2.45\%$ and $97.90 \pm 4.00\%$, respectively. The relative error was 0.65% and 2.10%, and the relative standard deviation was 2.47% and 4.09%, respectively (Table 1). These results indicated the reliability and excellent performance of the DAC-ELISA.

3.4. DAC-ELISA optimization in assay development

The aforementioned experiments were conducted under optimized conditions. The selection of optimal substrate concentration and the determination of the substrate incubation time are presented in the subsequent section.

Identifying an appropriate substrate concentration is essential in this method because it determines the background signal (noise) level for the negative control, which can substantially influence the sensitivity of the assay. It is a trade-off between the substrate

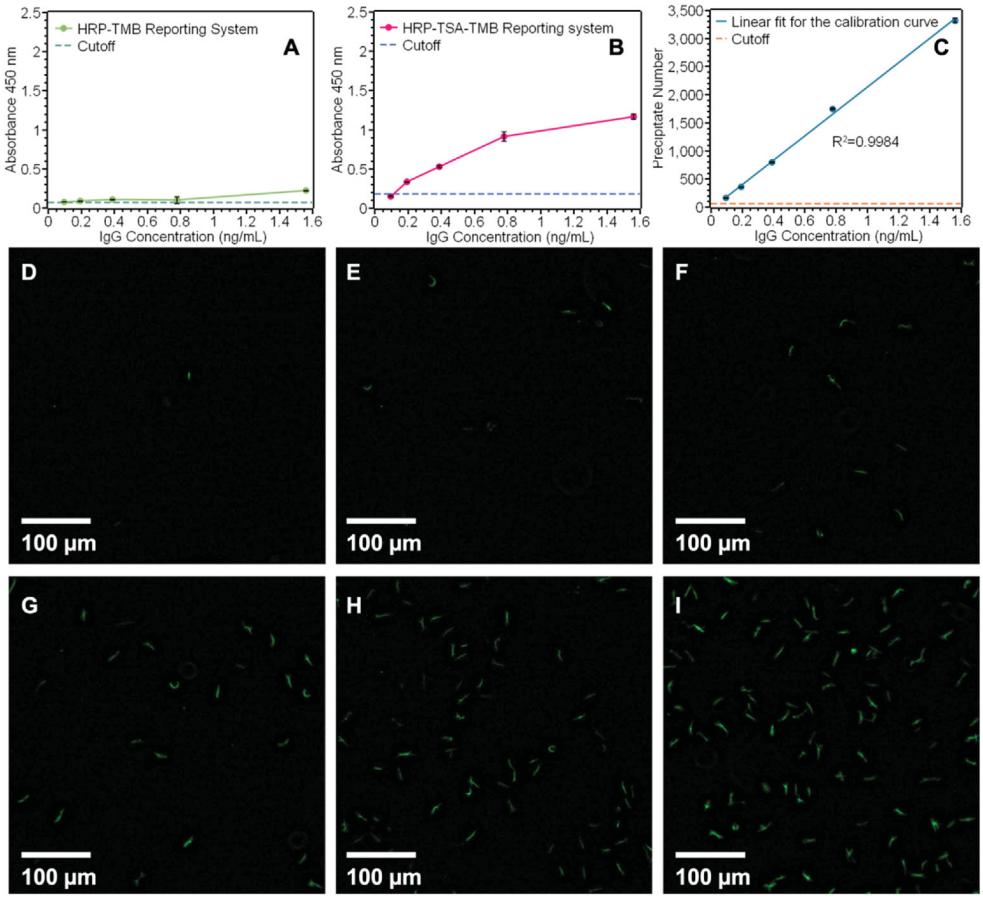

Fig. 3. Performance of DADC reporting system for mouse IgG detection. IgG detection using (A) HRP-TMB reporting system, (B) HRP-TSA-TMB reporting system, and (C) DAC reporting system. One representative image at each IgG concentration - (D) 0 (negative control), (E) 0.0977 ng/mL, (F) 0.1953 ng/mL, (G) 0.3906 ng/mL, (H) 0.7813 ng/mL, (I) 1.5625 ng/mL - was used to establish the calibration curve of DAC-ELISA system.

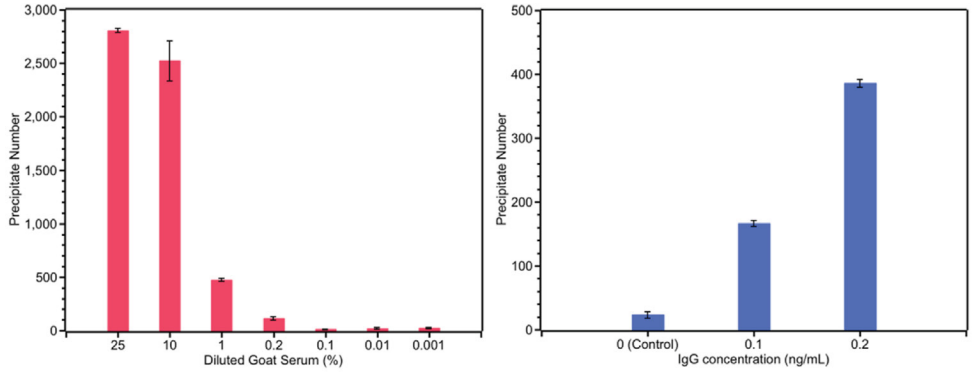

Fig. 4. Matrix effect and recovery tests of DAC-ELISA. (A) Background signal from mouse-IgG free goat serum at varied dilutions, and (B) Recovery tests using mouse IgG spiked into 100,000 × diluted goat serum with the final concentrations of 0 ng/mL (control), 0.2 ng/mL, and 0.1 ng/mL (n = 3).

Table 1
Performance of DAC-ELISA in the recovery tests. Mouse IgG standards spiked into 100,000-fold diluted goat serum (n = 3).

Target Molecule	Reference concentration (ng/mL)	Detected Concentration (ng/mL)	Relative Error (RE%)	Reproducibility (RSD%)	Recovery (%)
Mouse IgG	0.2	0.1987 ± 0.0049	0.65	2.47	99.35 ± 2.45
Mouse IgG	0.1	0.0979 ± 0.0040	2.10	4.09	97.90 ± 4.00

concentration and the precipitate formation (rapidness and countability). On the one hand, a higher substrate concentration results in considerable numbers of ELFA precipitates to be generated in a short time. However, more precipitates (noise) for negative control

decline the signal-to-noise ratio and consequently decrease the sensitivity of the assay. On the other hand, too low substrate concentration requires extended assay time to form precipitates. In the current study, four substrate concentrations ranging from 12.5 μM to 50 μM were tested with an incubation time of 2.5 h. As illustrated in Fig. S3, the numbers of ELFA precipitates decreased with the decrease of concentrations of ELFP. At the concentration of 50 μM (Fig. S3A), a higher number of precipitates were produced but intertwined with each other, which causes difficulty in counting accuracy. Once the concentration was equal to or lower than 16.67 μM (Figs. S3C and D), it is observed that nearly no ELFA precipitate appeared, which was an ideal situation for the negative control. Therefore, 16.67 μM ELFP solution (ELFA saturated) was used in the assay.

Conducting the assay with a proper substrate incubation time is significant as well. Being similar to the effect of substrate concentration on the performance, it is also a trade-off between substrate incubation time and the precipitate formation (rapidness and count-ability). On the one hand, a short substrate incubation time may result in insufficient ELFA precipitates produced, which causes the failure of the assay. On the other hand, excessive ELFA precipitates associated with extended incubation time intertwine with each other and then form aggregates, resulting in counting inaccuracy and underestimating the precipitate number. In addition, a long incubation time is not desired since it indicates a long assay time for the results. To determine a suitable substrate incubation time, a time lapsing study lasting 4 h was conducted to monitor the precipitate layout on the well bottom. As illustrated in Fig. 5, ELFA precipitates began to appear after 1 h incubation, and its number increased gradually with the incubation time to 2 h. However, 3 h incubation results in abundant ELFA precipitates with a few precipitates intertwined, and the intertwinement becomes more significant with 4 h incubation (Fig. 5C and D). To maximize the number of ELFA precipitates for a better sensitivity while minimizing the intertwinement of precipitates for better counting accuracy, 2.5 h incubation time was used in the assay development.

3.5. Discussion

A dual amplification enabled counting system was integrated with conventional plate-based ELISA for enhanced assay performance. TSA significantly enriches the number of ALP on one antigen-antibody binding event, while ALP-enabled fluorescent precipitate formation allows direct-counting of the precipitates for concentration correlation of target molecules. One-step ALP single amplification was also tested under the similar experimental conditions and all IgG concentrations returned nearly no fluorescent precipitates. It is attributed to the fact that the number of the ALP is not enough to produce detectable signal. Therefore, TSA plays a critical role in the dual amplification system.

To shorten the assay time and enhance the sensitivity, ELFA-saturated ELFP substrate solution is employed in conjunction with the optimal substrate concentration and incubation time. Under the optimal conditions, detection of mouse IgG with high

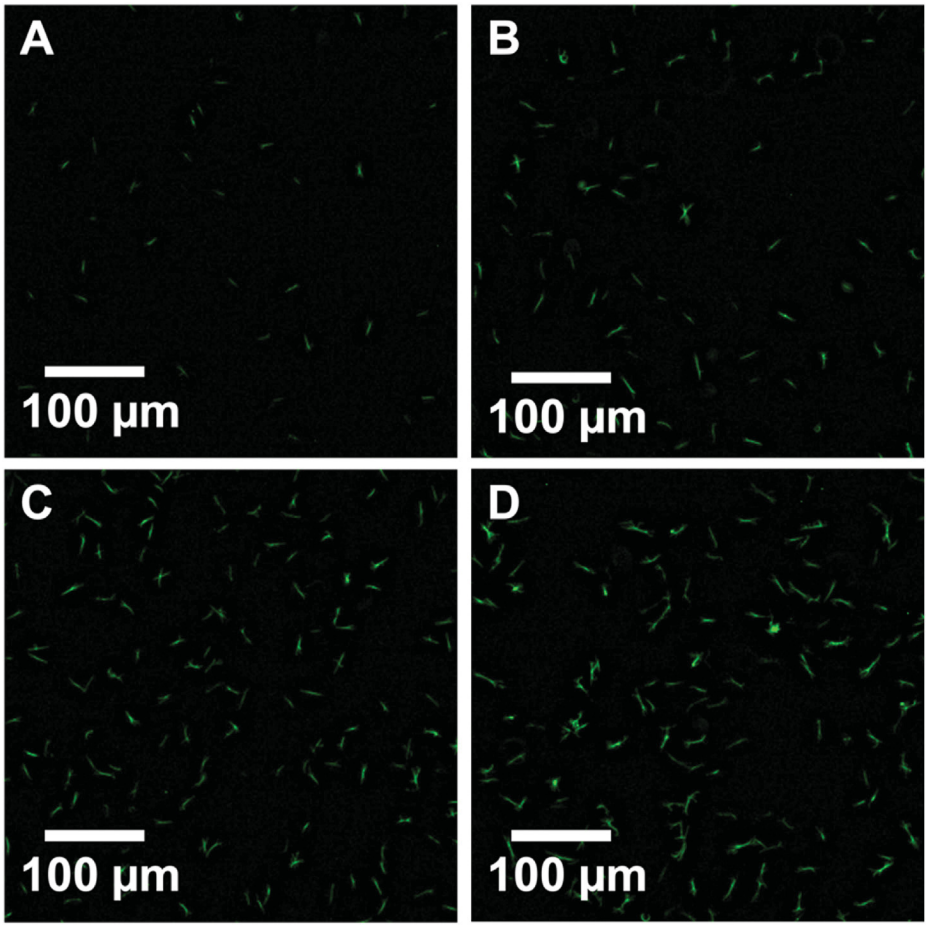

Fig. 5. Determination of the substrate incubation time. One representative image for different incubation times at (A) 1 h, (B) 2 h, (C) 3 h, and (D) 4 h, respectively. The analyte was IgG standard with a concentration of 1.5625 ng/mL. The substrate was 16.67 μM ELFP solution (ELFA saturated), and the dual amplification protocol was applied.

sensitivity, accuracy, and precision was obtained. Current protocol is adequate for real applications, corroborated by the good recovery test result using spiked samples. However, it is worth pointing out that only 25 images were captured for each well in the current practice, and the number of ELFA precipitates in these 25 images was employed to represent the signal for concentration correlation. The main rationale relies on the relatively uniform distribution of ELFA precipitates across the well, indicating there is no need to conduct time-consuming whole well scanning. As shown in Figs. S4 and 25 images at five different spots in a well were captured (Fig. S4A). Counting results of these five spots were employed to conduct the single-factor ANOVA test. The *p*-value was 0.07, indicating no significant difference among the different spots tested. The other rationale of only capturing 25 images (instead of the whole well) is to consider the time required for image capturing. It takes about 50 s to capture 25 images, while it requires about 7 min to scanning each whole well. Considering the triplicated experiments on multiple IgG concentrations in each round, it could take hours to complete the scanning of all wells if whole well scanning were used. This could cause a significant difference in incubation time at different wells for imaging and the corresponding precipitate number as the enzymatic reaction is a continuous process, thus sacrificing the assay accuracy. The utilization of quenching reagents to terminate the enzymatic reaction like conventional ELISA was also exploited. Ethylenediaminetetraacetic acid (EDTA) and L-phenylalanine are two inhibitors that are widely employed for ALP [35]. The addition of these inhibitor solutions, if successful, could quench the enzymatic reaction, thus allowing direct-counting of the whole well without the aforementioned issue. However, our study shows that the distribution of the ELFA precipitates is disturbed extensively by the addition of bulk quenching solution, resulting in inaccuracy in counting. Moreover, more time is required for the disturbed precipitates to completely settle down again, resulting in a longer assay time. Therefore, the quenching reagent was not introduced in the final protocol to terminate the enzymatic reaction. In addition, to further shorten the turnaround time of the entire assay, strategies are not limited to the optimization of the assay steps conducted in this study. All other classic ELISA optimization strategies such as varying the capture/detection antibody concentrations, finding the shortest blocking time, etc. could be applied to the current assay.

The DAC reporting system possesses several prominent advantages compared to colorimetric signal detection. The counting based signal detection strategy can overcome the intrinsic resolution limitation of the instrumentation, which is the major barrier of the conventional plate-based ELISA. Although the introduction of additional signal amplification strategies such as TSA and nanoparticles into plate-based ELISA, this barrier is not fully resolved as the signal detection principle remains the same. On the contrary, employing the image-based direct-counting method substantially avoid such issue. The sensitivity of the fluorescent microscope is so high that individual ELFA precipitates at the well bottom are detected and contribute to a higher sensitivity. The dual amplification enabled direct-counting based ELISA system has enormous potential as it is compatible with any commercial ELISA kit and any other type of ELISA. The prerequisites for accomplishing the DAC-ELISA are an optically transparent surface for supporting ELFA precipitates from DAC-ELISA, the HRP-labeled detection antibody as a catalyst for TSA, the SA-ALP as the reporter enzyme, and a fluorescent microscope with scanning function and an appropriate filter. All these instruments/reagents are commercially available and highly accessible in any advanced analytical laboratory. The concentrations of B-T, SA-ALP, ELFP substrates can be adjusted according to the need for detection sensitivity and the assay time. Another highlight of the DAC-ELISA system is the convenience as all reagents are commercially available with quality control. Thus it does not require additional complicated synthesis as other nanoparticles-based strategies under laboratory development. Not limit to plate-based ELISA, the DAC reporting system can also be integrated with bead-based ELISA to develop a new digital detection technique with ultra-sensitivity. Nowadays, it is a mature technique to achieve one immunocomplex on individual magnetic beads [36,37]. The TSA amplification only occurs to the bead bearing individual immunocomplex without crossing reaction onto other beads since the short lifetime of tyramide radicals when the concentration of beads is low [38]. In addition, ELFA precipitates tend to localize at the enzymatic activity sites rather than diffusing to other places [33,34]. Combining these merits together, DAC-based ELISA is promising. One big advantage of this method is that there is no compartmentalization required compared with the existed digital ELISA. Also, current beads based digital ELISA typically requires a high binding affinity between antibody-antigen pairs with a K_D value usually below 10^{-12} to survive through rigorous washing steps [39]. However, in the present study, IgG antibody typically possesses a K_D value in the nM range and the results indicate that the developed dual amplification enabled counting based system may be applicable for antibody-antigen pairs with low affinity. Besides the aforementioned appealing attributes in DAC-ELISA, some downsides still remain compared to conventional colorimetric ELISA. One limitation is the relatively long assay time. By introducing the dual amplification and counting step into the conventional ELISA, the assay time is elongated compared to conventional ELISA. The other limitation is that the image capturing time by a scanning microscope is longer than the absorbance reading time by a microplate reader. Absorbance readouts obtained by a microplate reader for multiple wells are typically less than 1 min, while the image capturing under current practice is over 10 min. This limitation can be addressed if snapshot based on-chip imaging techniques are developed, which can image a large area or even the entire microplate wells in seconds. Overall, the present study of the DAC-ELISA system opens an avenue in developing high-performance biomarker assays with high sensitivity, accuracy, and precision, and it holds great potential to fight diseases.

4. Conclusion

ELISA is the predominant technique in the detection of biomarkers and the diagnosis of various diseases. Notwithstanding its ubiquity and numerous advantages, its low sensitivity greatly limits its application in quantitative detection of low abundant biomarkers in order to accomplish the earlier diagnosis. To bridge the gap between the need and availability, an innovative dual amplification enabled digital-counting based ELISA (DADC-ELISA) was developed and validated for ultrasensitive detection of biomarkers using mouse total IgG as a model compound. The dual amplification strategy was accomplished through the combination of tyramide signal amplification and alkaline phosphatase enabled formation of fluorescent precipitates, while the rapid counting of fluorescent precipitates can correlate the number to the concentration of IgG with a good linearity. Under the optimal conditions, the limit of detection of the commercial mouse IgG kit (1.56 ng/mL) can be extended to an impressive limit of detection (LOD) of 54.5 pg/mL. Recovery tests were further carried out to demonstrate the reliability of the developed method. Due to its compatibility with conventional plate-based ELISA, the developed dual amplification strategy opens a new and universal avenue to improve the sensitivity of conventional plate-based ELISA and holds great potential in achieving ultrasensitive detection of biomarkers on conventional plate-based ELISA platform.

CRediT authorship contribution statement

Haomin Liu: Formal analysis, Writing – original draft, conducts the experiments, analyzes the data, and draft the manuscript, while. **Yu Lei:** Project initiation and, Writing – review & editing, initiates the project, designs the experimental procedure, and revises the manuscript.

Declaration of competing interest

The authors declare that they have no known competing financial interests or personal relationships that could have appeared to influence the work reported in this paper.

Acknowledgements

YL greatly appreciates the partial support from NSF. HML thanks Shaojia Yang for the help with graph design and Shiyao Wang for helpful discussion. HML was also partially supported by a fellowship grant from GE's Industrial Solutions Business Unit under a GE-UConn partnership agreement. The views and conclusions contained in this document are those of the authors and should not be interpreted as necessarily representing the official policies, either expressed or implied, of Industrial Solutions or UConn.

Appendix A. Supplementary data

Supplementary data to this article can be found online at https://doi.org/10.1016/j.aca.2022.339510.

References

[1] I.A. Darwish, Immunoassay methods and their applications in pharmaceutical analysis: basic methodology and recent advances, Int. J. Biomed. Sci. IJBS 2 (2006) 217.
[2] G.A. Bonwick, C.J. Smith, Immunoassays: their history, development and current place in food science and technology, Int. J. Food Sci. Technol. 39 (2004) 817–827.
[3] E. Engvall, P. Perlmann, Enzyme-linked immunosorbent assay, Elisa. J. Immunol. 109 (1972) 129. LP – 135.
[4] S.G. Gundersen, I. Haagensen, T.O. Jonassen, K.J. Figenschau, N. De Jonge, A.M. Deelder, Magnetic bead antigen capture enzyme-linked immunoassay in microtitre trays for rapid detection of schistosomal circulating anodic antigen, J. Immunol. Methods 148 (1992) 1–8.
[5] S.T. Gaylord, T.L. Dinh, E.R. Goldman, G.P. Anderson, K.C. Ngan, D.R. Walt, Ultrasensitive detection of ricin toxin in multiple sample matrixes using single-domain antibodies, Anal. Chem. (2015), https://doi.org/10.1021/acs.analchem.5b00322.
[6] D.M. Rissin, C.W. Kan, T.G. Campbell, S.C. Howes, D.R. Fournier, L. Song, T. Piech, P.P. Patel, L. Chang, A.J. Rivnak, E.P. Ferrell, J.D. Randall, G.K. Provuncher, D.R. Walt, D.C. Duffy, Single-molecule enzyme-linked immunosorbent assay detects serum proteins at subfemtomolar concentrations, Nat. Biotechnol. 28 (2010) 595–599, https://doi.org/10.1038/nbt.1641.
[7] X. Wang, L. Cohen, J. Wang, R. Walt, Competitive immunoassays for the detection of small molecules using single molecule arrays, J. Am. Chem. Soc. 140 (2018) 18132–18139, https://doi.org/10.1021/jacs.8b11185. D.
[8] R. Gerbers, W. Foellscher, H. Chen, C. Anagnostopoulos, M. Faghri, A new paper-based platform technology for point-of-care diagnostics, Lab Chip 14 (2014) 4042–4049, https://doi.org/10.1039/C4LC00786G.
[9] D. Wu, J. Zhang, F. Xu, X. Wen, P. Li, X. Zhang, S. Qiao, S. Ge, N. Xia, S. Qian, X. Qiu, A paper-based microfluidic Dot-ELISA system with smartphone for the detection of influenza A, Microfluid. Nanofluidics 21 (2017), https://doi.org/10.1007/s10404-017-1879-6.
[10] A.N. Berlina, A.V. Zherdev, B.B. Dzantiev, ELISA and lateral flow immunoassay for the detection of food colorants: state of the art, Crit. Rev. Anal. Chem. 49 (2019) 209–223, https://doi.org/10.1080/10408347.2018.1503942.
[11] L. Wu, G. Li, X. Xu, L. Zhu, R. Huang, X. Chen, Application of nano-ELISA in food analysis: recent advances and challenges, TrAC Trends Anal. Chem. (Reference Ed.) 113 (2019) 140–156, https://doi.org/10.1016/j.trac.2019.02.002.
[12] H.T. Al-Jighefee, H.M. Yassine, M.A. Al-Nesf, A.A. Hssain, S. Taleb, A.S. Mohamed, H. Maatoug, M. Mohamedali, G.K. Nasrallah, Evaluation of antibody response in symptomatic and asymptomatic COVID-19 patients and diagnostic assessment of new IgM/IgG ELISA kits, Pathog, https://doi.org/10.3390/pathogens10020161, 2021.
[13] V. Roy, S. Fischinger, C. Atyeo, M. Slein, C. Loos, A. Balazs, C. Luedemann, M.G. Astudillo, D. Yang, D.R. Wesemann, R. Charles, A.J. Lafrate, J. Feldman, B. Hauser, T. Caradonna, T.E. Miller, M.R. Murali, L. Baden, E. Nilles, E. Ryan, D. Lauffenburger, W.G. Beltran, G. Alter, SARS-CoV-2-specific ELISA development, J. Immunol. Methods 484–485 (2020) 112832, https://doi.org/10.1016/j.jim.2020.112832.
[14] D.A. Giljohann, C.A. Mirkin, Drivers of biodiagnostic development, Nature 462 (2009) 461.
[15] J.M. Barletta, D.C. Edelman, N.T. Constantine, Lowering the detection limits of HIV-1 viral load using real-time immuno-PCR for HIV-1 p24 antigen, Am. J. Clin. Pathol. 122 (2004) 20–27.
[16] P.R. Srinivas, B.S. Kramer, S. Srivastava, Trends in biomarker research for cancer detection, Lancet Oncol. 2 (2001) 698–704.
[17] Y. Gao, Y. Zhou, R. Chandrawati, Metal and metal oxide nanoparticles to enhance the performance of enzyme-linked immunosorbent assay (ELISA), ACS Appl. Nano Mater. 3 (2020) 1–21, https://doi.org/10.1021/acsanm.9b02003.
[18] A.D. Kurdekar, L.A.A. Chunduri, C.S. Manohar, M.K. Haleyurgirisetty, I.K. Hewlett, K. Venkataramaniah, Streptavidin-conjugated gold nanoclusters as ultrasensitive fluorescent sensors for early diagnosis of HIV infection, Sci. Adv. 4 (2018) 1–11, https://doi.org/10.1126/sciadv.aar6280.
[19] M.S. Tabatabaei, R. Islam, M. Ahmed, Applications of gold nanoparticles in ELISA, PCR, and immuno-PCR assays: a review, Anal. Chim. Acta 1143 (2021) 250–266, https://doi.org/10.1016/j.aca.2020.08.030.
[20] M. Lu, Q. He, Y. Zhong, J. Pan, Z. Lao, M. Lin, T. Wang, X. Cui, J. Ding, S. Zhao, Ultrasensitive colorimetric assay based on a multi-amplification strategy employing Pt/IrO2@SA@HRP nanoflowers for detection of progesterone in saliva samples, Anal. Methods (2021), https://doi.org/10.1039/d1ay00053e.
[21] Y. Huang, H. Liu, W. Chen, M.-P. Nieh, Y. Lei, Genetically engineered bionanoparticles with co-expressed enzyme reporter and recognition element for IgG immunoassay, Sensor. Actuators Rep. 1 (2019) 100003, https://doi.org/10.1016/j.snr.2019.100003.
[22] A.P. Acharya, P.M. Nafisi, A. Gardner, J.L. MacKay, K. Kundu, S. Kumar, N. Murthy, A fluorescent peroxidase probe increases the sensitivity of commercial ELISAs by two orders of magnitude, Chem. Commun. 49 (2013) 10379–10381, https://doi.org/10.1039/c3cc44783a.
[23] M.N. Bobrow, T.D. Harris, K.J. Shaughnessy, G.J. Litt, Catalyzed reporter deposition, a novel method of signal amplification application to immunoassays, J. Immunol. Methods 125 (1989) 279–285, https://doi.org/10.1016/0022-1759(89)90104-X.
[24] G. Mayer, M. Bendayan, Biotinyl-tyramide: a novel approach for electron microscopic immunocytochemistry, J. Histochem. Cytochem. 45 (1997) 1449–1454, https://doi.org/10.1177/002215549704501101.
[25] X. Qian, R.V. Lloyd, Recent developments in signal amplification methods for in situ hybridization, Diagn. Mol. Pathol. 12 (2003) 1–13, https://doi.org/10.1097/00019606-200303000-00001.
[26] S. Roy, H.D. Axelrod, K.C. Valkenburg, S. Amend, K.J. Pienta, Optimization of prostate cancer cell detection using multiplex tyramide signal amplification, J. Cell. Biochem. 120 (2019) 4804–4812, https://doi.org/10.1002/jcb.28016.
[27] L. Yuan, L. Xu, S. Liu, Integrated tyramide and polymerization-assisted signal amplification for a highly-sensitive immunoassay, Anal. Chem. 84 (2012) 10737–10744, https://doi.org/10.1021/ac302439v.
[28] A.M. Maley, P.M. Garden, D.R. Walt, Simplified digital enzyme-linked immunosorbent assay using tyramide signal amplification and fibrin hydrogels, ACS Sens. 5 (2020) 3037–3042, https://doi.org/10.1021/acssensors.0c01661.
[29] Z. Huang, E. Terpetschnig, W. You, R.P. Haugland, 2-(2′-Phosphoryloxyphenyl)-4(3H)-quinazolinone derivatives as fluorogenic precipitating substrates of phosphatases, Anal. Biochem. 207 (1992) 32–39, https://doi.org/10.1016/0003-2697(92)90495-S.
[30] S.T. Dyhrman, Phosphate stress in cultures and field populations of the dino agellate, Society 65 (1999) 3205–3212.
[31] T. Matsushita, Y.Y. Chan, A. Kawanami, G. Balmes, G.E. Landreth, S. Murakami, Extracellular signal-regulated kinase 1 (ERK1) and ERK2 play essential roles in osteoblast differentiation and in supporting osteoclastogenesis, Mol. Cell Biol. 29 (2009) 5843–5857, https://doi.org/10.1128/mcb.01549-08.
[32] J. Nedoma, A. Štrojsová, J. Vrba, J. Komárková, K. Šimek, Extracellular phosphatase activity of natural plankton studied with ELF97 phosphate: fluorescence quantification and labelling kinetics, Environ. Microbiol. 5 (2003) 462–472, https://doi.org/10.1046/j.1462-2920.2003.00431.x.
[33] V.B. Paragas, J.A. Kramer, C. Fox, R.P. Haugland, V.L. Singer, The ELF®-97 phosphatase substrate provides a sensitive, photostable method for labelling cytological targets, J. Microsc. 206 (2002) 106–119, https://doi.org/10.1046/j.1365-2818.2002.01017.x.
[34] H. Liu, Y. Huang, Y. Lei, A whole area scanning–enabled direct-counting strategy for studying blocking efficiency in mitigating protein-solid surface binding, Anal. Bioanal. Chem. (2021) 1493–1502, https://doi.org/10.1007/s00216-020-03120-7.
[35] R.L. Dean, Kinetic studies with alkaline phosphatase in the presence and absence of inhibitors and divalent cations, Biochem. Mol. Biol. Educ. 30 (2002) 401–407, https://doi.org/10.1002/bmb.2002.494030060138.
[36] L. Song, D. Shan, M. Zhao, B.A. Pink, K.A. Minnehan, L. York, M. Gardel, S. Sullivan, A.F. Phillips, R.B. Hayman, D.R. Walt, D.C. Duffy, Direct detection of bacterial genomic DNA at sub-femtomolar concentrations using single molecule arrays, Anal. Chem. 85 (2013) 1932–1939, https://doi.org/10.1021/ac303426b.
[37] Q. Zhang, X. Zhang, J. Li, H. Gai, Nonstochastic protein counting analysis for

precision biomarker detection: suppressing Poisson noise at ultralow concentration, Anal. Chem. 92 (2020) 654–658, https://doi.org/10.1021/acs.analchem.9b04809.
[38] K. Akama, K. Shirai, S. Suzuki, Droplet-free digital enzyme-linked immunosorbent assay based on a tyramide signal amplification system, Anal. Chem. 88 (2016) 7123–7129, https://doi.org/10.1021/acs.analchem.6b01148.
[39] L. Chang, D.M. Rissin, D.R. Fournier, T. Piech, P.P. Patel, D.H. Wilson, D.C. Duffy, Single molecule enzyme-linked immunosorbent assays: theoretical considerations, J. Immunol. Methods 378 (2012) 102–115, https://doi.org/10.1016/j.jim.2012.02.011.